

**Modeling the oxygen K absorption in the interstellar medium: an
XMM-Newton view of Sco X-1**

J. García^{1,2}, J.M. Ramírez³, T.R. Kallman², M. Witthoef², M.A. Bautista¹, C. Mendoza⁴,

P. Palmeri⁵,

and

P. Quinet^{5,6}

Received _____; accepted _____

¹Department of Physics, Western Michigan University, Kalamazoo, MI 49008, USA

`javier.garcia@wmich.edu, manuel.bautista@wmich.edu`

²NASA Goddard Space Flight Center, Greenbelt, MD 20771

`timothy.r.kallman@nasa.gov, michael.c.witthoeft@nasa.gov`

³Astrophysikalisches Institut Potsdam, An der Sternwarte 16 D-14482 Potsdam, Germany

`jramirez@aip.de`

⁴Centro de Física, IVIC, Caracas 1020A, Venezuela

`claudio@ivic.ve`

⁵Astrofysique et Spectroscopie, Université de Mons - UMONS, B-7000 Mons, Belgium

`palmeri@umh.ac.be`

⁶IPNAS, Sart Tilman B15, Université de Liège, B-4000 Liège, Belgium

`quinet@umh.ac.be`

ABSTRACT

We investigate the absorption structure of the oxygen in the interstellar medium by analyzing *XMM-Newton* observations of the low mass X-ray binary Sco X-1. We use simple models based on the O I atomic cross section from different sources to fit the data and evaluate the impact of the atomic data in the interpretation of astrophysical observations. We show that relatively small differences in the atomic calculations can yield spurious results. We also show that the most complete and accurate set of atomic cross sections successfully reproduce the observed data in the 21 – 24.5 Å wavelength region of the spectrum. Our fits indicate that the absorption is mainly due to neutral gas with an ionization parameter of $\xi = 10^{-4}$ erg cm s⁻¹, and an oxygen column density of $N_{\text{O}} \approx 8 - 10 \times 10^{17}$ cm⁻². Our models are able to reproduce both the K edge and the K α absorption line from O I, which are the two main features in this region. We find no conclusive evidence for absorption by other than atomic oxygen.

1. Introduction

X-ray spectroscopy provides a powerful tool for understanding the physical and chemical properties of the diffuse interstellar medium (ISM). The X-ray band covers the emission and absorption spectra produced by inner-shell transitions of the most abundant ions from carbon to iron. The interaction of X-ray photons from bright point sources such as galactic X-ray binaries with the ISM imprints absorption lines and edges in the spectrum of the source. The energy position and the shape of these features depend on whether the absorption is due to free atoms or molecules, and on whether these atoms or molecules are in the gas or in the solid phase.

Neutral oxygen is a major constituent of the ISM, which makes it one of the most important elements in astronomical observations. Precise knowledge of the neutral oxygen atomic quantities is needed for the correct modeling of the observed spectra. Theoretical calculations of the photoabsorption cross section of the ground state of O I were carried out by McLaughlin & Kirby (1998) (hereafter MCK98), using the *R*-matrix method, giving a detailed comparison with the experimental results of Stolte et al. (1997). Although they claimed overall agreement, there are significant discrepancies in the positions of the inner-shell excited resonances, and the near threshold resonance profiles. This problem was overcome with the LS-coupling calculation of Gorczyca & McLaughlin (2000) (hereafter GMC00), by taking into account core relaxation effects and the smearing of the K-edge due to Auger damping. A more complete *R*-matrix calculation was carried out in intermediate coupling by García et al. (2005) (hereafter GAR05), for all the ions in the oxygen isonuclear sequence. There is very good agreement between of the GAR05 calculations with both the experimental cross section (Stolte et al. 1997), and the GMC00 results.

Oxygen inner-shell features in the X-ray spectrum of galactic sources have been used to provide abundance determinations in the ISM as well as estimates of the oxygen ionization fractions (Schulz et al. 2002; Takei et al. 2002; Juett et al. 2004; Turner et al. 2004; Ueda et al. 2005; Juett et al. 2006). However, studies in the IR and UV have shown that oxygen can also be found as solid particles (Draine 2003; Whittet 2003). It has been argued that oscillatory modulations near the K edge should be detected, known as X-ray absorption fine structure (XAFS). These are condensed matter modulations of the atomic cross section due to the presence of solid particles (Lee & Ravel 2005; Lee et al. 2009). Studies of the soft X-rays from galactic sources have reported possible detections of XAFS signatures (Paerels et al. 2001; Lee et al. 2001, 2002; de Vries et al. 2003; Ueda et al. 2005; de Vries & Costantini 2009; Kaastra et al. 2009; Pinto et al. 2010).

XMM-Newton observations of the X-ray source Scorpius X-1 (Sco X-1), reveal strong absorption in the wavelength region corresponding to neutral oxygen. Located at ~ 2.8 kpc distance (Bradshaw et al. 1999), and with a flux of $F \sim 3.4 \times 10^8$ erg cm $^{-2}$ s $^{-1}$ (in the 2 – 10 keV energy band), it is the brightest X-ray source in the sky, other than the Sun and the diffuse X-ray background radiation. Its high X-ray flux provides very good statistics in relatively short exposure times, giving the opportunity to study signatures of oxygen absorption in the ISM with great detail. de Vries et al. (2003) analyzed high resolution X-ray spectra of the reflection grating spectrometer (RGS) of the *XMM*-Newton satellite for several galactic sources, including Sco X-1. By comparing low and high extinction sources they were able to separate the ISM and the instrumental components of the O I K edge. de Vries & Costantini (2009) searched for XAFS signatures in the spectrum of Sco X-1. The XAFS signature is derived from the differences between the observed flux and the flux predicted theoretically. However, the model used by these authors is based on the atomic oxygen absorption cross section calculated by MCK98.

In this Letter we show the importance of the accuracy of the atomic data used to model the details of the oxygen absorption in the ISM. We show that small differences in the K edge structure derived from different atomic calculations yield spurious results when applied to astronomical observations. In Section 2 we describe the observational data used for our study, while the theoretical models are described in Section 3. The results derived from the fits of the models to the data are presented in Section 4. Finally, the main conclusions are summarized in Section 5.

2. Observation and Data reduction

For the purpose of this work, we make use of the *XMM*-Newton spectrum of Sco X-1, taken on orbit 0592 (Obs ID=0152890101), with the RGS instrument (den Herder et al.

2001). The general observational strategy is described in detail in de Vries et al. (2003) and de Vries & Costantini (2009), and will not be described here. Given the high X-ray flux of Sco X-1, standard spectroscopy mode would lead to very high level of pile-up. This was avoided by choosing a faster readout mode, which is able to read each one of the nine RGS CCDs in separate exposures. Because of a failure in the RGS2, we make use of only the RGS1 data in what follows. During this observation there were 24 separate contiguous exposures; but only the fifth and the eighteenth contain calibrated and reliable data in the 21 – 25 Å spectral range. Thus, we only use these exposures through the spectral analysis. In the notation of the SAS `rgsproc` task, these two exposures are labeled as S005 and S018. We follow the standard procedure for the reduction and extraction of the RGS spectrum using SAS version 10, with the latest calibration files (CCFs). We finally present the spectrum with the default binning of 0.05 Å, making use of the full resolution of the spectrometer.

3. The Models

3.1. Atomic data

Figure 1 shows the photoabsorption cross section for the ground state of neutral oxygen in the 22.5-24 Å wavelength region from the calculations by MCK98, GMC00, and GAR05. All these curves have been convolved with a 182 meV full width at half maximum Gaussian, in order to match the resolution of the curves presented in GMC00. This spectral region covers both the K edge near 22.5 Å and the $K\alpha$ 1s-2p absorption line near 24.5 Å. Besides the differences in the position of $K\alpha$, the GAR05 and GMC00 calculations agree very well. Nevertheless, there are significant discrepancies with respect to the MCK98 result, particularly in the shape of the K edge and in the energy separation between the K-edge and the $K\alpha$ resonance. Because the $K\alpha$ absorption is a prominent and well resolved feature

in the spectra, and its energy is experimentally known, it is used as reference in all spectral fits. Thus, uncertainties in the energy and shape of the cross section used around the inner-shell edges are reflected in the form of spurious residuals in the fits across the edges.

These differences have been addressed in detail by GMC00 as being due to two important effects: the relaxation of the orbitals due the vacancy in the K shell (which affects the atomic structure, and thus the resonances and edge positions), and the decay of the resonances to an infinite number of channels via spectator Auger decay (which affects the widths of the resonances). It is evident from the comparison in Figure 1 that the lack of these two effects underestimates the absorption cross section near the K edge by 20-50%.

3.2. Model A

In order to describe the features observed in the Sco X-1 observation we have made use of the photoionization code `XSTAR`. Several calculations were carried out covering a range of parameters, the most important being the hydrogen column density N_{H} , and the ionization parameter, defined as $\xi = L/nR^2$, where L is the luminosity of the source, R its distance, and n is the density of the gas (Tarter et al. 1969). We have constructed a grid of `XSTAR` models covering hydrogen column densities of $N_{\text{H}} = 10^{19} - 10^{22} \text{ cm}^{-2}$, ionization parameters of $\xi = 10^{-4} - 10 \text{ erg cm}^{-2} \text{ s}^{-1}$, with the gas density fixed to $n = 10^3 \text{ cm}^{-3}$. The spectral region of interest is relatively small and includes the wavelength range $21 - 24.5 \text{ \AA}$, where only oxygen ions are relevant. Thus, the `XSTAR` models include hydrogen, helium and oxygen ions in the ionization balance calculation, assuming an oxygen abundance relative to hydrogen of $A_{\text{O}} = 6.8 \times 10^{-4}$ (Grevesse & Sauval 1998). We will refer to this model as Model A. The `XSTAR` models incorporate the GAR05 cross sections for all the charge states of oxygen.

3.3. Models B, C and D

A simpler description of the absorption of X-rays by a cold medium is to assume that all the spectral features are a result of photoabsorption by only O I. Then, the observed flux can be approximated as

$$F(E) = F_0 \exp[-N_{\text{O I}} \sigma_{\text{O I}}(E)] \quad (1)$$

where F_0 is a normalization factor, $N_{\text{O I}}$ is the oxygen column density, and $\sigma_{\text{O I}}(E)$ is the photoabsorption cross section for neutral oxygen. This is a convenient way to evaluate the relevance of the atomic data used to fit the observation. Using this assumption, we have produced 3 additional models using Equation 1, each one with a different cross section available from the literature. Model B includes the R -matrix calculations by McLaughlin & Kirby (1998) (MCK98), Model C includes the photoionization calculations by García et al. (2005) (GAR05), and Model D includes the Gorczyca & McLaughlin (2000) cross section (GMC00). Note that the XSTAR calculation, Model A, and Model C are equivalent in the sense that they use the same atomic data, although the XSTAR calculation includes the background due to H and He. These models are summarized in Table 1.

4. Results

We have used the models described in Section 3 to fit the absorption observed in the X-ray spectrum of Sco X-1. To fit the models to the observation and determine the corresponding statistics we use the X-ray spectral package XSPEC v.12.3.0. All the fits presented here are carried out in the 21 – 24.5 Å spectral region. Figure 2 shows the fit using Model A. This is our main model, since it results from a self-consistent photoionization calculation and incorporates the most recent atomic cross section for O I (GAR05). In the upper panel, the black and gray data points correspond to exposures S005 and S018,

respectively. The best-fit using the XSTAR photoionization model (Model A), is shown in solid lines, with red and blue corresponding to the fit applied to each exposure, respectively. The spectrum shows a very strong atomic K edge which covers the 22.8 – 23.3 Å wavelength range. The inner-shell $K\alpha$ absorption resonance at ~ 23.5 Å is also one of the strongest features in the spectra. The $K\beta$ resonance absorption is much weaker, but still detectable at ~ 22.9 Å. In the lower panel, we show the residuals with respect to the model, in units of σ . Black and gray points correspond to exposures S005 and S018, respectively. Model A fits the K edge and the $K\alpha$ absorption line successfully in the two exposures of Sco X-1. The statistics for the combined fit (i.e., for the two exposures), shows a reduced chi-squared of $\chi^2/\text{dof} = 2.75620$ (where dof is the number of degrees of freedom). The best-fit hydrogen column density is $N_{\text{H}} = 1.33 \times 10^{21} \pm 0.02 \text{ cm}^{-2}$, which corresponds to a oxygen column density of $N_{\text{O}} = 9.04 \times 10^{17} \pm 0.12 \text{ cm}^{-2}$.

In order to investigate in more detail the effects of the atomic data into the description of the observed spectra, we repeated the fit to the same observation using simple models based on the raw photoabsorption cross section of neutral oxygen (see Equation 1). In Figure 3 we show the fits to the Sco X-1 spectrum using Models B and C. In the upper panel of the Figure, the black/gray data points are the observation, while the red/blue curves are the models corresponding to exposures S005/S018, respectively. The best-fits using Models B and C are shown with dashed and solid lines, respectively. The middle panel shows the residuals in units of σ with respect to Model B, and the lower panel shows residuals with respect to Model C. It is important to notice that if these two models were equivalent, the dashed and solid lines with the same color should be close to each other. However, there is a clear discrepancy between the dashed lines (Model B) and the solid lines (Model C), in the region near the K edge of oxygen ($\sim 22.5 - 23$ Å). These differences are clearly seen in the residuals of the fit for Model B, shown in the middle panel. The residuals also show that Model B cannot completely fit the intensity of the $K\alpha$ absorption line at

$\sim 23.5 \text{ \AA}$. This model predicts an oxygen column density of $N_{\text{O}} = 9.25 \times 10^{17} \pm 0.07 \text{ cm}^{-2}$, and the statistics of the fit gives a reduced chi-squared of $\chi^2/\text{dof} = 6.02484$, which is much worse than the previous fit using the full photoionization calculation with XSTAR (Model A). As expected, the fit using the raw cross section of GAR05 (Model C), is equivalent to the fit using Model A, giving a reduced chi-squared of $\chi^2/\text{dof} = 2.44650$. Model C predicts an oxygen column density of $N_{\text{O}} = 7.94 \times 10^{17} \pm 0.22 \text{ cm}^{-2}$, somewhat smaller than for Models A and B. The difference between Models A and C may be due to the numerical interpolation used in the storage and retrieval of the cross sections by XSTAR.

Model B, which is based on the MCK98 atomic cross section, is the same model used by de Vries & Costantini (2009) to fit the oxygen absorption in the spectrum of Sco X-1. These authors claimed the detection of XAFS signatures in the spectra, based on the relative changes in the observed flux with respect to the smooth flux predicted by the model, for energies above the K edge. They also argued that the apparent shift of the observed edge with respect to the atomic model could be due to the fact that some fraction of the oxygen in the ISM is bound in solids. Nevertheless, the analysis presented here shows that the large residuals found while fitting (Model B) are artifacts of the use of the MCK98 cross section.

Finally, in Figure 3 we show a similar comparison, using the GAR05 and the GMC00 cross sections (Models C and D). As before, the upper panel shows the Sco X-1 spectrum and the best-fit models. The black/gray data points are the observation, while the red/blue curves are the models corresponding to exposures S005/S018, respectively. The best-fits using Models C and D are shown with solid and dashed lines, respectively. The middle and lower panels show the residuals in units of σ for Models D and C. The two models are equivalent, giving similar fits ($\chi^2/\text{dof} = 2.76445$, for Model D). This is consistent with the agreement between the calculations by GMC00 and GAR05. The oxygen column density derived from this model ($N_{\text{O}} = 10.49 \times 10^{17} \pm 0.06 \text{ cm}^{-2}$), is larger than in all the previous

models, but consistent within the uncertainties of the parameters predicted by Models A-C. The difference in the predicted O column between Models C and D can be explained by the differences in the cross sections. In this small spectral region, the O column depends almost exclusively on the depth of the K-edge. By comparing the values of the cross section shown in at 22.8 and 23.0 Å (i.e., before and after the K-edge) in Figure 1, one can notice that the K-edge in the GMC00 curve is weaker than in the GAR05 curve. Therefore, weaker features require a larger column density to reproduce the data. All the models applied here, and the parameters derived from the corresponding fits are summarized in Table 1.

In all the fits presented here, we see residuals of around $\pm 2\sigma$ distributed homogeneously along the entire spectral range considered in our analysis, consistent with the reduced chi-squared close to 2 obtained in our best fit. This suggest that most of the errors of the fit are systematic. However, we notice significant residuals at wavelengths shorter than the $K\alpha$ line. Coincidentally, by looking the O I experimental cross section (Stolte et al. 1997), we can see a rather intense and broad feature at 23.35 Å, which is due to the $1s \rightarrow \pi^*$ resonance in molecular oxygen. Unfortunately, a gap in the 23.33 – 23.44 Å wavelength region of the observation forbids further analysis. Nevertheless, we cannot rule out the presence of molecules in this observation.

5. Conclusions

In this Letter we have shown the relevance of the atomic data in modeling the X-ray spectra from cosmic sources. In particular, we have modeled the Sco X-1 spectrum as viewed by the RGS1 instrument on board of the *XMM* Newton satellite, covering the 21 – 24.5 Å wavelength region. The main spectral features in this region are the absorption K edge and $K\alpha$ line from neutral oxygen. The absorption occurs when the X-rays interact with the cold neutral gas of the ISM. We found a good fit using a self-consistent photoionization

model, which includes the most recent atomic data calculations for the oxygen isonuclear sequence by GAR05. Our fits indicate that the absorbing gas has an ionization parameter of $\xi = 10^{-4}$ erg cm s⁻¹ and a hydrogen column density of $N_{\text{O}} \approx 8 - 10 \times 10^{17}$ cm⁻²

Simple models based on the raw atomic photoabsorption cross section of O I from three different theoretical calculations were used to evaluate the impact of their accuracy. We show that models based on the MCK98 atomic cross sections are unable to reproduce the structure of the K edge in detail, while models based on the GMC00 and GAR05 atomic data provide a much accurate fit to the main features observed in the spectrum. The fits using the most up to date models do not show evidence for absorption by anything other than atomic oxygen.

The analysis presented here indicates that the atomic data uncertainties in combination with the limited resolution of the grating spectra makes detection of molecular or solid material challenging. Although oxygen is expected to be found in molecular form or locked into solids in the ISM, the use of accurate atomic calculations to correctly account for atomic oxygen is crucial when searching for XAFS or similar features in the X-ray spectra of astronomical sources.

We thank T. Gorczyca for providing the MCK98 and GMC00 calculations. This work was supported by a grant from the NASA astrophysics theory program 05-ATP05-18. This research has made use of NASA's Astrophysics Data System.

REFERENCES

- Bautista, M. A., & Kallman, T. R. 2001, *ApJS*, 134, 139
- Bradshaw, C. F., Fomalont, E. B., & Geldzahler, B. J. 1999, *ApJ*, 512, L121
- de Vries, C. P., & Costantini, E. 2009, *A&A*, 497, 393
- de Vries, C. P., den Herder, J. W., Kaastra, J. S., Paerels, F. B., den Boggende, A. J., & Rasmussen, A. P. 2003, *A&A*, 404, 959
- den Herder, J. W., et al. 2001, *A&A*, 365, L7
- Draine, B. T. 2003, *ARA&A*, 41, 241
- García, J., Mendoza, C., Bautista, M. A., Gorczyca, T. W., Kallman, T. R., & Palmeri, P. 2005, *ApJS*, 158, 68
- Gorczyca, T. W., & McLaughlin, B. M. 2000, *J. Phys. B: At. Mol. Opt. Phys.*, 33, L859
- Grevesse, N., & Sauval, A. J. 1998, *Space Sci. Rev.*, 85, 161
- Juett, A. M., Schulz, N. S., & Chakrabarty, D. 2004, *ApJ*, 612, 308
- Juett, A. M., Schulz, N. S., Chakrabarty, D., & Gorczyca, T. W. 2006, *ApJ*, 648, 1066
- Kaastra, J. S., de Vries, C. P., Costantini, E., & den Herder, J. W. A. 2009, *A&A*, 497, 291
- Lee, J. C., Ogle, P. M., Canizares, C. R., Marshall, H. L., Schulz, N. S., Morales, R., Fabian, A. C., & Iwasawa, K. 2001, *ApJ*, 554, L13
- Lee, J. C., & Ravel, B. 2005, *ApJ*, 622, 970
- Lee, J. C., Reynolds, C. S., Remillard, R., Schulz, N. S., Blackman, E. G., & Fabian, A. C. 2002, *ApJ*, 567, 1102

- Lee, J. C., Xiang, J., Ravel, B., Kortright, J., & Flanagan, K. 2009, *ApJ*, 702, 970
- McLaughlin, B. M., & Kirby, K. P. 1998, *Journal of Physics B Atomic Molecular Physics*, 31, 4991
- Paerels, F., et al. 2001, *ApJ*, 546, 338
- Pinto, C., Kaastra, J. S., Costantini, E., & Verbunt, F. 2010, *A&A*, 521, A79+
- Schulz, N. S., Cui, W., Canizares, C. R., Marshall, H. L., Lee, J. C., Miller, J. M., & Lewin, W. H. G. 2002, *ApJ*, 565, 1141
- Stolte, W. C., et al. 1997, *Journal of Physics B Atomic Molecular Physics*, 30, 4489
- Takei, Y., Fujimoto, R., Mitsuda, K., & Onaka, T. 2002, *ApJ*, 581, 307
- Tarter, C. B., Tucker, W. H., & Salpeter, E. E. 1969, *ApJ*, 156, 943
- Turner, A. K., Fabian, A. C., Lee, J. C., & Vaughan, S. 2004, *MNRAS*, 353, 319
- Ueda, Y., Mitsuda, K., Murakami, H., & Matsushita, K. 2005, *ApJ*, 620, 274
- Whittet, D. C. B., ed. 2003, *Dust in the galactic environment*

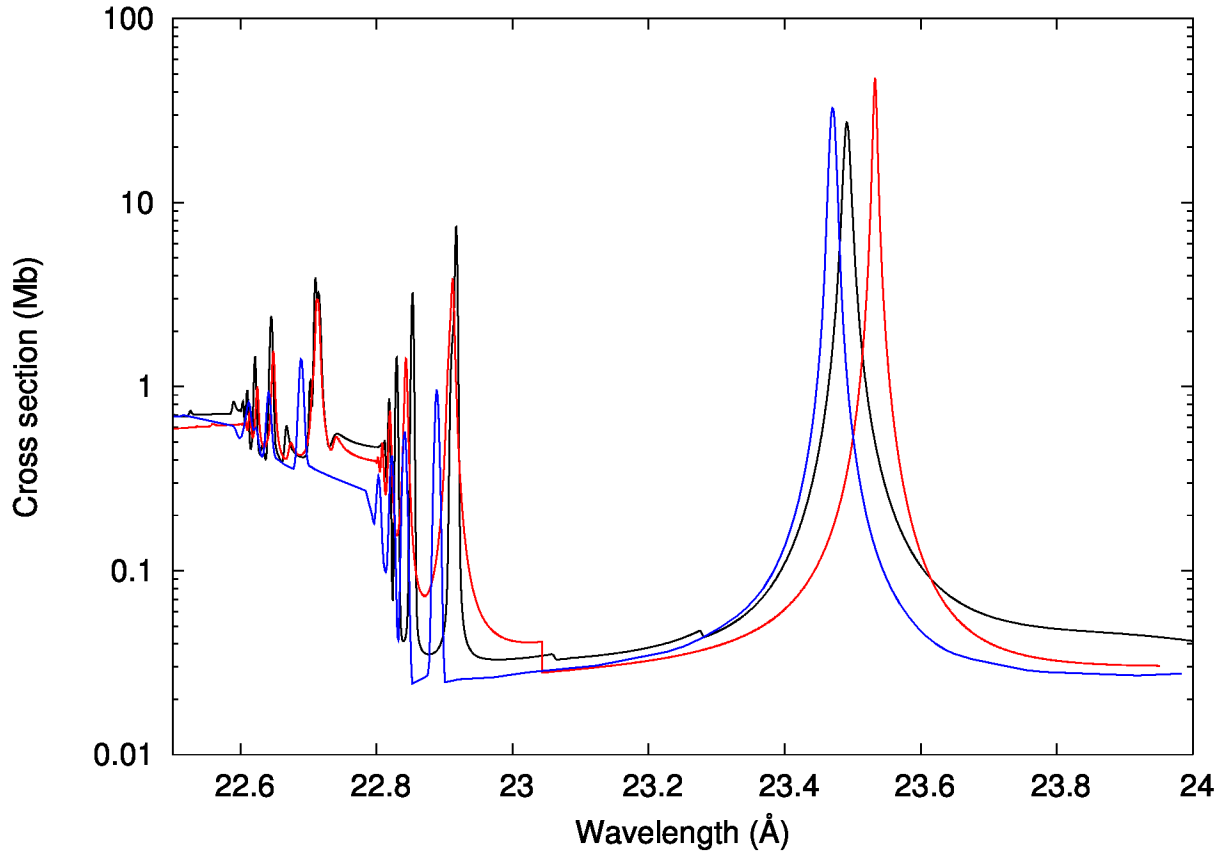


Fig. 1.— Comparison of the theoretical photoabsorption cross sections for neutral oxygen in the 22.5-24 Å wavelength region from McLaughlin & Kirby (1998) (blue curve), Gorczyca & McLaughlin (2000) (red curve), and García et al. (2005) (black curve). This spectral region covers both the absorption K-edge and the $K\alpha$ absorption line (1s-2p) from O I. All the curves have been convoluted with a 182 meV FWHM Gaussian.

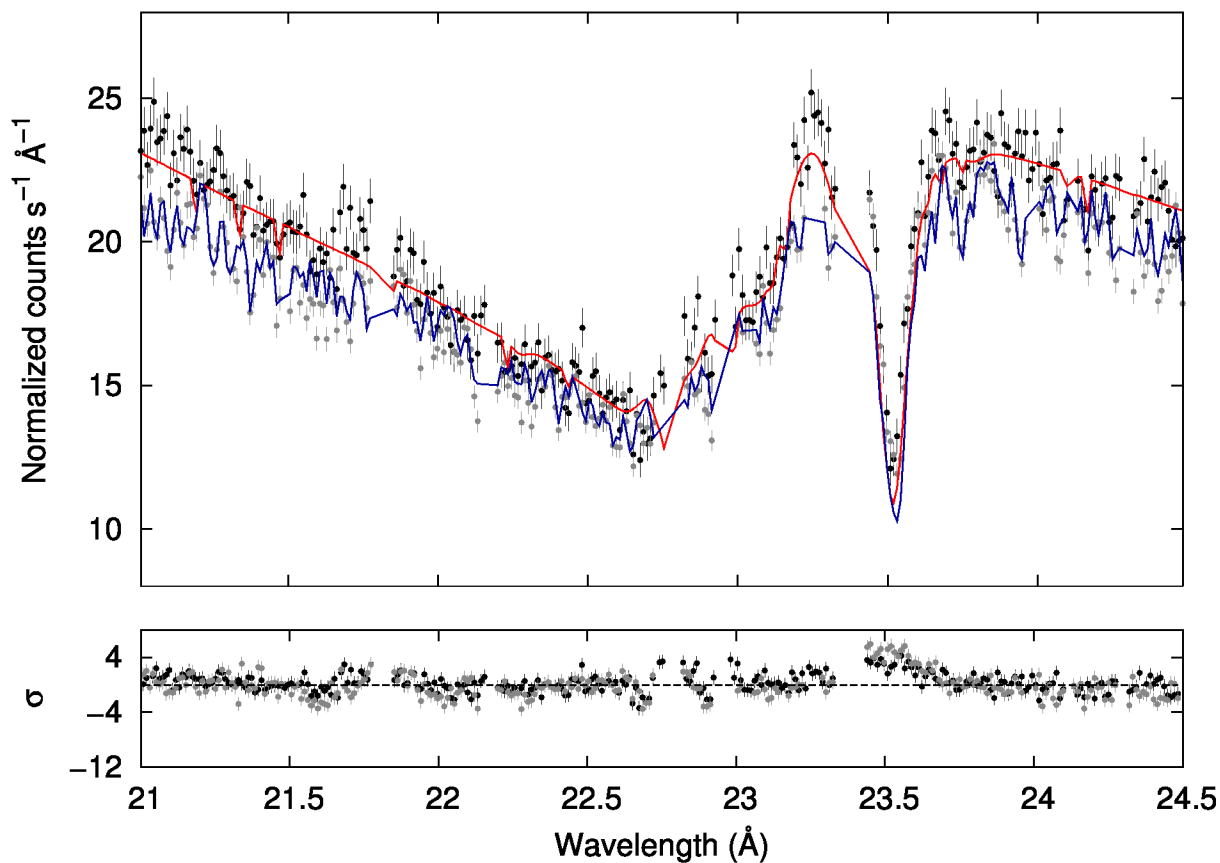


Fig. 2.— Sco X-1 spectrum as viewed by RGS1 in *XMM* Newton, covering the 21 – 24.5 Å wavelength region. In the upper panel, the black and gray data points correspond to exposures S005 and S018, respectively, while the best-fit using the *xstar* photoionization model (Model A), is shown in red and blue applied to each exposure, respectively. The lower panel shows the residuals in units of σ in the same range with respect to the model. Black and gray points correspond to exposures S005 and S018, respectively.

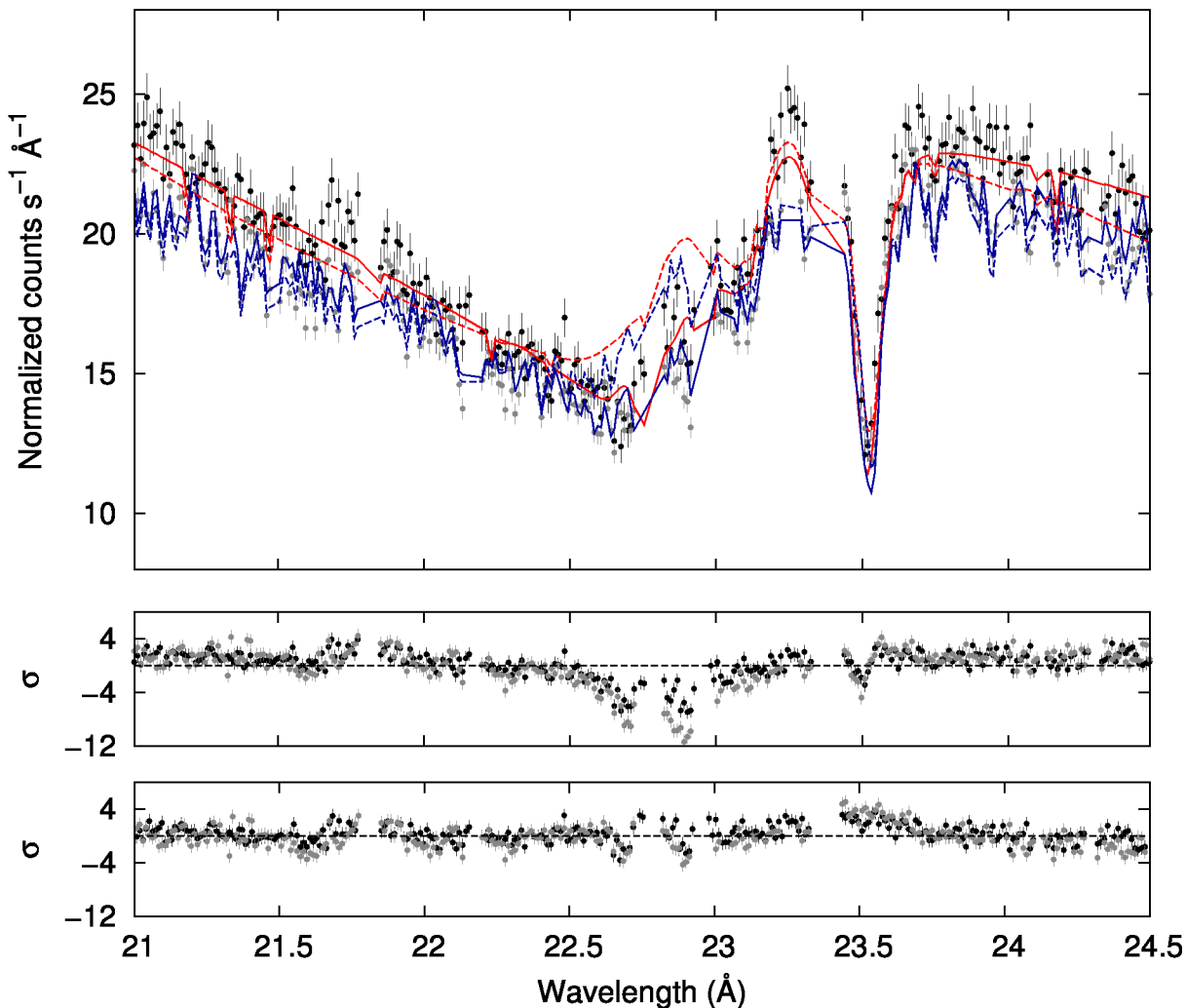


Fig. 3.— Comparison of the spectral fitting using two different models. Upper panel: Sco X-1 spectrum as viewed by RGS1 in *XMM* Newton, covering the 21 – 24.5 Å wavelength region. The black/gray data points are the data while the red/blue curves are the models corresponding to exposures S005/S018, respectively. The best-fits using Models B and C are shown with dashed and solid lines, respectively. Middle panel: residuals in units of σ with respect to Model B. Lower panel: residuals in units of σ with respect to Model C.

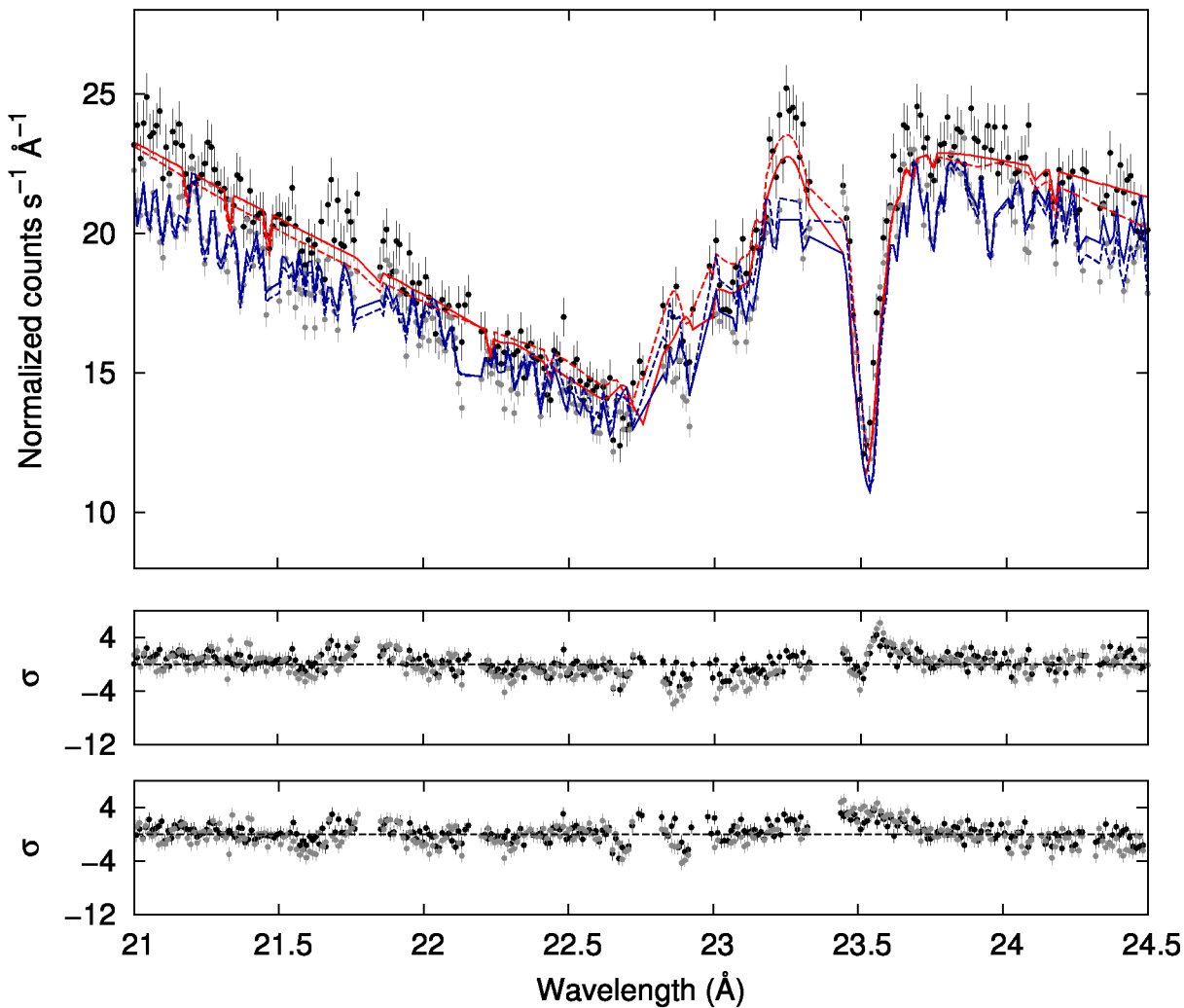


Fig. 4.— Comparison of the spectral fitting using two different models. Upper panel: Sco X-1 spectrum as viewed by RGS1 in *XMM* Newton, covering the 21 – 24.5 Å wavelength region. The black/gray data points are the data while the red/blue curves are the models corresponding to exposures S005/S018, respectively. The best-fits using Models C and D are shown with solid and dashed lines, respectively. Middle panel: residuals in units of σ with respect to Model D. Lower panel: residuals in units of σ with respect to Model C.

Table 1. List of Models

Model	Description	Atomic Data	N_{O} (10^{17} cm^{-2})	χ^2/dof	Notes
A	Full XSTAR model	AKA01 ^a +GAR05 ^b	9.04 ± 0.12	2.75620	No significant residuals
B	Atomic Cross Section ^e	MCK98 ^c	9.25 ± 0.07	6.02484	Large residuals near K edge
C	Atomic Cross Section ^e	GAR05 ^b	7.94 ± 0.22	2.44650	No significant residuals
D	Atomic Cross Section ^e	GMC00 ^d	10.49 ± 0.06	2.76445	No significant residuals

^aBautista & Kallman (2001)

^bGarcía et al. (2005)

^cMcLaughlin & Kirby (1998)

^dGorczyca & McLaughlin (2000)

^eSee Equation (1)